



# **NEW DESIGNS FOR EMBEDDED PASSIVE WIRELESS SENSORS**

Mehran Fallah Rad  
University of Manitoba, Canada

L. Shafai  
University of Manitoba, Canada

D. J. Thomson  
University of Manitoba, Canada

## **Abstract**

In this paper, a passive wireless strain sensor for structural health monitoring applications is presented. The embedded sensor consists of a metallic cavity connected to a radiating antenna element. The system requires no permanent physical connection and is activated from the surface of concrete. The metallic cavity is a resonator that changes dimension in response to an applied force. A short length of wire from the inside to the outside couples RF signals from the cavity to an antenna. The sensor can then be interrogated via the antenna. Such a system has the advantage of requiring no permanent physical connection between the sensor and the data acquisition unit (DAU). Changes in the structure's dimensions will be reflected as changes in the resonant frequency, which is then used to calculate the strain on the structure. This paper investigates new types of passive wireless sensor along with the antenna element designed to be embedded in concrete. A full parametric study of the sensor is performed using full wave simulators. The microwave sensor along with the radiating antennas have been fabricated and tested. Comparison of the fabrication and simulation data shows excellent agreement.

## **INTRODUCTION**

Recently, there have been few papers on wireless embedded sensors used as temperature-threshold and chloride-threshold indicators [1], moisture [2], and conductivity [3] measurement units. While, these sensors have shown promising results, no work has yet been done on strain measurements using embedded wireless sensors. The sensor investigated here consist of a resonant metallic cavity attached to a transmit/receive antenna. The antenna communicates with an external data acquisition unit [4] as shown in Fig. 1. The sensors are passive devices which require no permanent physical connections. Strain is measured by detecting shifts in resonant frequency of the resonator as a function of applied force. This shift is not necessarily linear and varies depending on the type of metallic resonator. In this paper, the wireless sensor is investigated in detail. The cavity resonator along with the radiating antenna element are explained along with some simulations and measurements done in the Antenna Laboratory of the University of Manitoba.

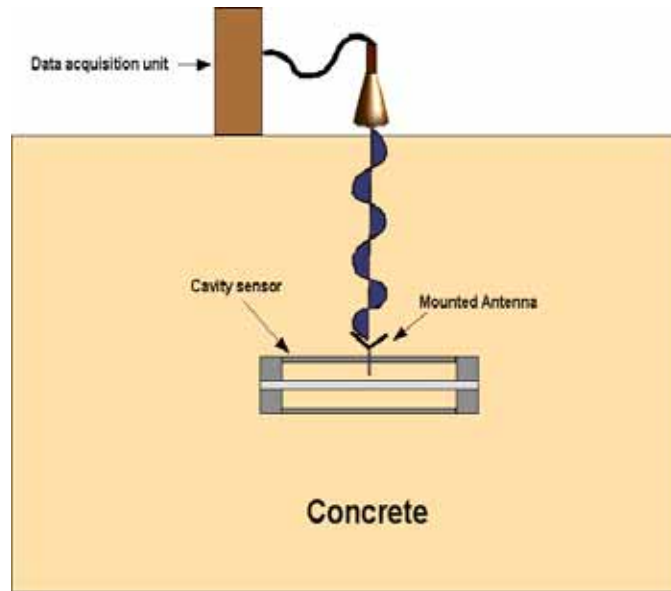


Figure 1. Geometry of the embedded sensor within concrete. The sensor is activated by the signal traveling through concrete. The signal is then sent back to the data acquisition unit by the mounted antenna.

## HELICAL CAVITY RESONATOR

The fabricated cavity resonator is shown in Fig. 2a. This is a tunable helical cavity resonator which consists of a helical inner conductor and a movable end wall. This cavity is fabricated from copper which has lower losses compared with other metals.

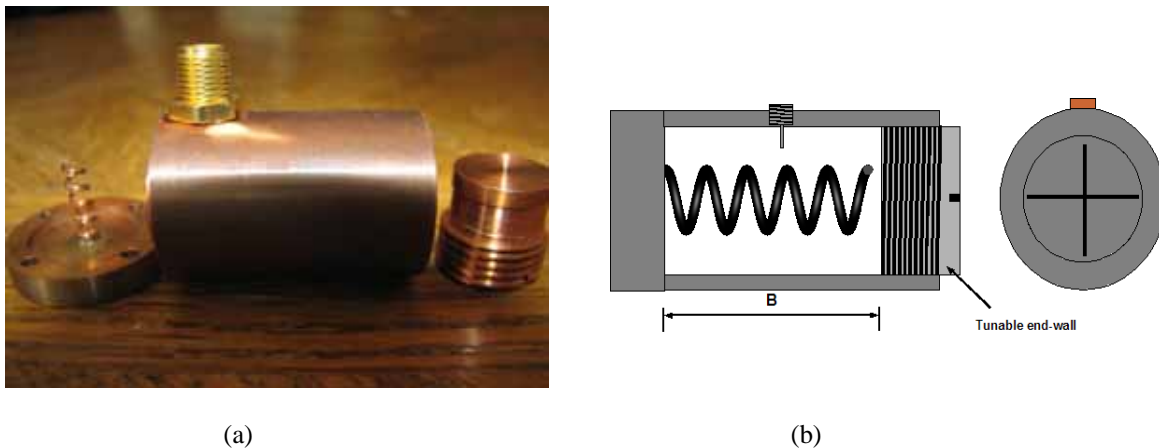


Figure 2. (a) Geometry of the fabricated helical resonator (disassembled). The antenna is mounted on top of the cavity. Signal enters into the cavity through the gold color connector (b) Drawing of the helical cavity resonator. Turning the end wall clockwise moves the wall in thus reducing the cavity length ( $B$ ).

The length of this cavity is variable as shown in Fig. 2b. This variation in length ( $B$ ) causes variations in resonant frequency of the resonator. In reality, the length of the cavity will change depending on the applied force (strain within concrete). This in turn will result in a shift in resonant frequency which is detected by the data acquisition unit. To illustrate, we manually changed the length of cavity by moving the end wall and recording changes in resonant frequency. Fig. 3 displays resonant frequency as a function of cavity length ( $B$ ). Note that for end wall positions near the helical inner conductor, the change in resonant frequency is much more rapid. This is the area in which the sensor will be operating.

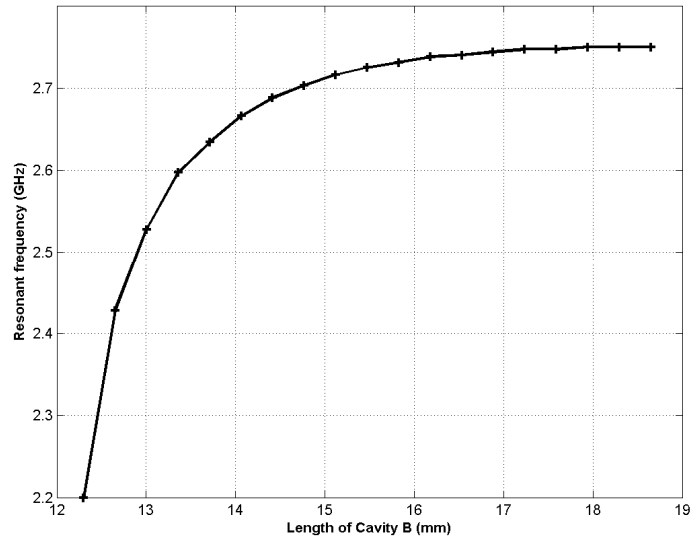


Figure 3. Shift in resonant frequency vs. length of cavity (B). At 12.3 mm, the end wall is moved in as much as possible and is almost touching the helical inner conductor.

Although in real applications the movements are in micro-strain, this resonator is expected to operate in the linear range of the slope with reasonable frequency shifts. For a given strain, shifts in resonant frequency are three times greater than previous fabricated cavities.

## EMBEDDED ANTENNA DESIGN

Another important part of our investigation is the embedded antenna. The sensors (cavity resonator and antenna) are typically embedded in concrete at a depth greater than 100 mm. Almost all the antennas available are designed to operate in free space (air) environment. Embedding the antenna or placing any type of material on its surface will change the properties of the antenna. These properties include the resonant frequency, radiation pattern, and gain. The gain of an antenna describes its ability to radiate power in a particular direction and takes the antenna losses and efficiency into consideration. Higher antenna gain means higher signal levels at the data acquisition unit.

For our application a planar antenna (microstrip antenna) which has light weight, low volume, and low cost of fabrication was investigated. The geometry of this antenna along with its radiation pattern is shown in Fig. 4. Typical gain values of microstrip antennas radiating in air are 4-7 dBi. Note that the antenna radiates outwards in a plane perpendicular to the surface of antenna. The radiation pattern in Fig. 4, was obtained from a patch antenna radiating in free space. If the same antenna is embedded in concrete, the pattern will be distorted and in some cases the main radiation will not be perpendicular to the surface of the antenna (antenna will radiate horizontally). Additionally, the gain will drop significantly due to the production of unwanted surface waves and losses within concrete. Under such conditions, the data acquisition unit will not be able to communicate with the embedded sensor. The problem of radiation pattern distortion and gain are strongly dependent on the material properties of the environment (concrete) and the depth at which the antennas are embedded. Material properties of concrete (permittivity and losses) are strongly dependent on the moisture and humidity. Higher permittivity values (higher water content), lead to larger pattern distortion and lower gain values. A study of concrete properties [5] showed that concrete permittivity can vary between 6-10 depending on the humidity and water content. Therefore, during the rain season the antennas will have lower gain and distorted patterns due to higher permittivity values. This makes the design challenging, since we can not design an antenna for a particular concrete humidity and water content (permittivity). It is beneficial to fabricate an antenna that is least dependent on concrete properties and can operate at depths greater than 100 mm.

To study the effects of concrete on antenna properties, simulations were performed using Ansoft Designer which is based on the Method of Moments. Different antenna structures were studied however, due to restriction in the length of the paper, only two cases are presented here.

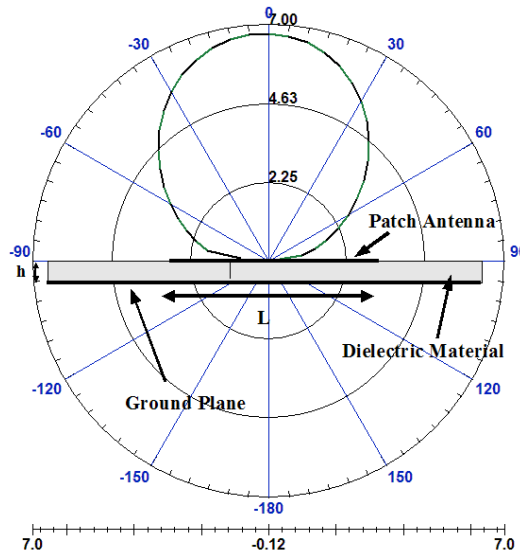


Figure 4. Geometry of a planar patch antenna along with its radiation pattern in polar co-ordinates

#### Simulated Antenna with Concrete Cover Layer

The geometry of a microstrip antenna placed underneath a concrete layer is shown in Fig. 5.

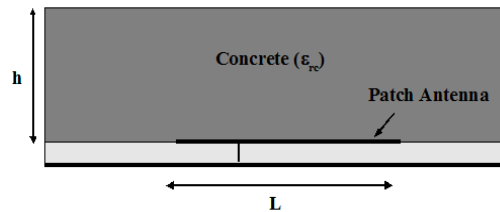


Figure 5. Geometry of the embedded patch antenna

The antenna length ( $L$ ) is 38 mm. The gain for the antenna vs. frequency is shown in Fig. 6. The gain of the reference antenna radiating in air is also plotted for comparison. Two different thicknesses of concrete ( $h$ ), 10 mm, and 20 mm are shown to indicate the gain distortion effect of concrete thickness. For concrete slab thicknesses larger than 1 mm, the gain drops significantly. This drop is more significant for wet concrete (permittivity  $\epsilon_r = 10$ ). Looking at Fig. 6, the reference antenna has a maximum gain of 7 dBi at a frequency of 2.45 GHz. The shift in frequency is evident as the concrete permittivity and depth is increased. The gain values drop as low as -12 dBi. For such cases, the peak of the radiation pattern is no longer in the vertical direction, and for certain cases it moves to the horizon.

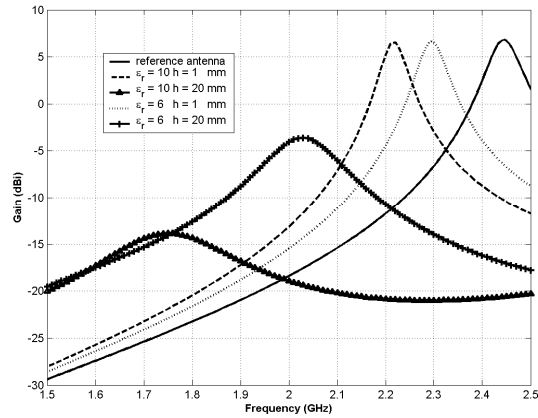


Figure 6. Gain vs. frequency for an embedded microstrip antenna. Note that maximum gain occurs at the resonant frequency of the antenna. The resonant frequency also moves as concrete permittivity is changed.

To correct the problem associated with the resonance shift, a layer of foam was inserted between the concrete and the surface of patch antenna (Fig. 7a). This will separate the antenna from the concrete and make the resonant frequency independent of concrete properties. However, the radiation pattern will still be distorted due to the production of unwanted power waves (surface waves) traveling within concrete. This is visible in the radiation pattern (gain plots) shown in Fig. 7a for a foam thickness of 10 mm. The gain plots are shown as a function of theta ( $\theta$ ). Note that  $\theta$  of zero (broadside) corresponds to the point perpendicular to the surface of the antenna and  $90^\circ$  corresponds to the point on the antenna plane. The gain plot of the reference antenna is very smooth with a maximum gain of 7 dBi at zero degrees. However, distortion is visible in the gain plots of the antenna embedded in concrete with different permittivity values. One can clearly see the gain drop when the antenna is placed adjacent to concrete. Beam splitting occurs for  $\epsilon_r$  of 7 and 8. The gain is particularly low (-2.13 dBi at broadside) for  $\epsilon_r$  of 8, with maximum beam at  $\theta = 57^\circ$ . Due to low gain values, it is obvious that a foam thickness of 10 mm is not sufficient at a concrete depth of 100 mm. Next, the foam thickness was increased to 60 mm with the gain plots shown in Fig. 7b.

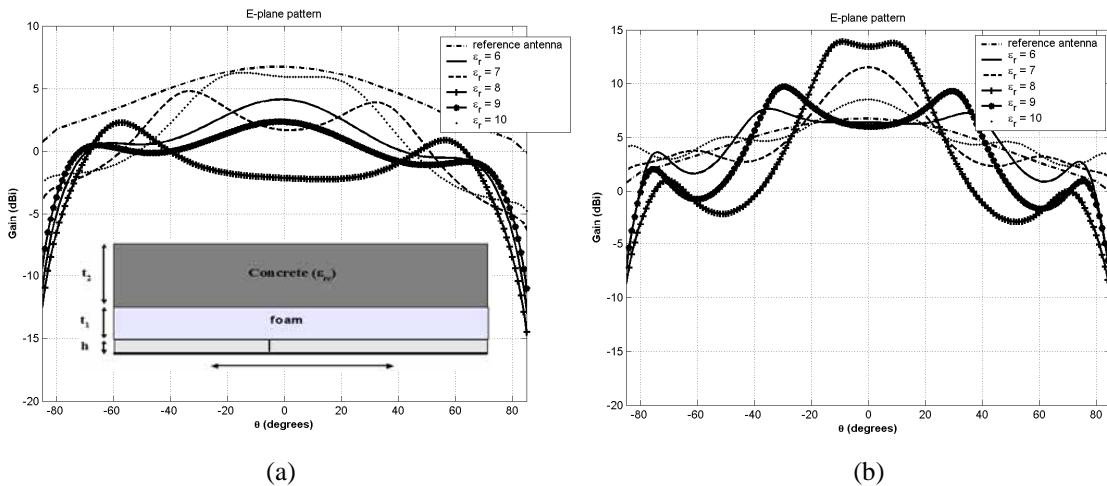


Figure 7. Radiation patterns of the antenna with foam cover layer (a)  $t_f=10$  mm, (b)  $t_f=12$  mm

Foam thickness of 60 mm corresponds to half wavelength at the operation frequency of 2.5 GHz. By selecting the correct foam thickness, a cavity that stores energy is created and this causes an increase in the gain values as shown

in Fig. 7b. Note that almost for all permittivity values in Fig. 7b, the gain at broadside is higher than the reference antenna. In one case the gain reaches as high as 14 dBi. The beam splitting effect is still visible in the radiation pattern plots. Unfortunately this effect can not be removed at the current depth (100 mm) at which the antenna is embedded.

### **Fabricated Embedded Antenna**

The simulated antennas shown in the previous section were fabricated and embedded within concrete. The fabricated antennas ready for concrete pour are shown in Fig. 8. The box on the left contains the antenna with a foam cover layer of 60 mm and the box on the right contains the antenna with a foam cover layer of 10 mm.



Figure 8. Fabricated antennas placed inside a wooden cast. The wires coming out of the box are used for gain measurements after the concrete has been poured.

Several tests were performed on the embedded antennas on different days after the concrete pour to measure the power radiated from the antennas. Unfortunately, due to weight restrictions, the radiation patterns of the antennas could not be measured in the Anechoic Chamber. Instead, the setup shown in Fig. 9 was used to measure the radiated power.

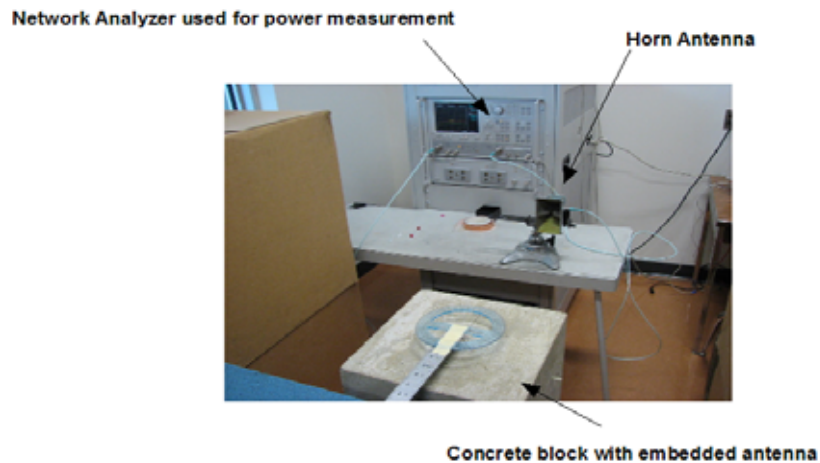


Figure 9. Setup used for power measurements

A horn antenna was used to transmit power to the embedded antennas within the concrete blocks. Power was delivered to the horn antenna via the SMA cable connected to port I of the Anritsu ME7808A network analyzer. The horn antenna radiates the electrical signal into the air which, is then picked up by the embedded antennas within

concrete. The wave power is then converted into an electrical signal which is detected by connecting port II of the network analyzer to the SMA cable connected to the embedded antennas within the concrete block. The setup shown in Fig. 9 rotates which allows us to measure the detected signal power for different angles. The normalized measured gain plots of the antenna with a 10 mm foam cover layer are shown in Fig. 10. Note that curve fitting was done to obtain smoother curves. Measurements were done on day 2, day 5 and day 40. The measured coupled power is normalized to the maximum value obtained on day 40. As expected, the signal level on day 2 is lower than day 40 by more than 2.3 dB. This is due to the moisture and water content within concrete. The difference between day 5 and day 40 is not as significant. Fig. 11 displays the same plots for the antenna with foam thickness of 60 mm. For this antenna, a larger difference of more than 3.5 dB between day 2 and day 40 is observed. This means that more than twice the power was detected on day 40. Therefore, we can clearly conclude that under high water conditions, almost half the power is lost within concrete due to losses.

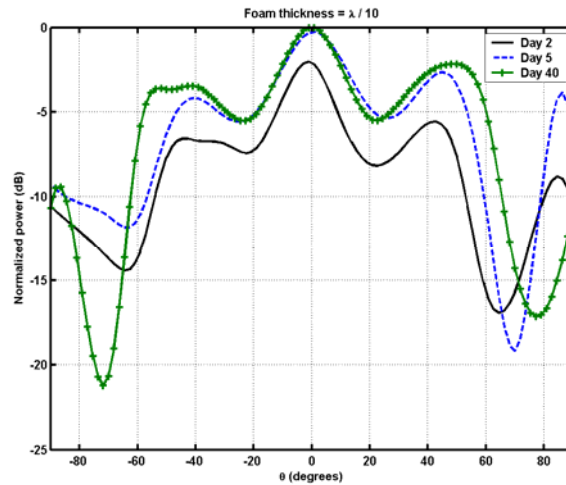


Figure 10. Measured coupled power for the embedded antenna, foam thickness of 10 mm

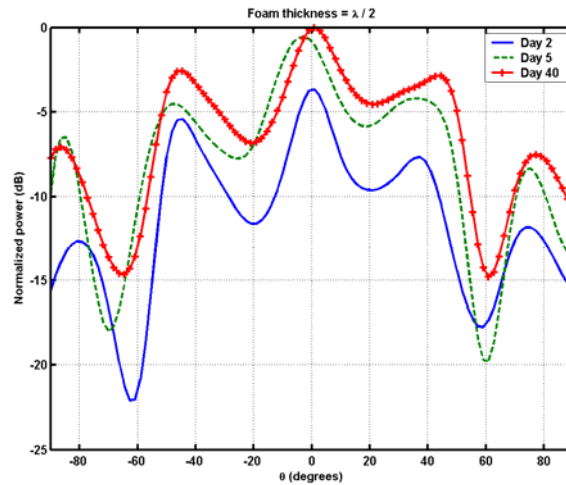


Figure 11. Measured coupled power for the embedded antenna, foam thickness of 60 mm

Finally, a comparison of the two antennas on day 2 and day 40 is shown in Fig. 12. The power plots are normalized to the maximum power that was measured (antenna with foam thickness of 60 mm). It is clear that the antenna with larger foam cover has better reception compared with the other case. A difference of more than 2.2 dB is seen on day 40. This is a significant number and will definitely affect the signal level at the data acquisition unit.

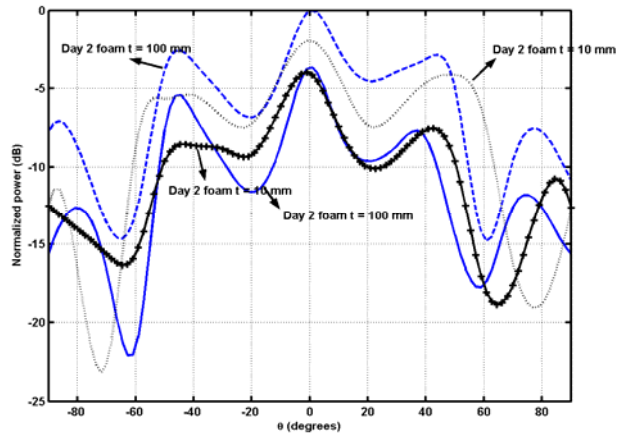


Figure 12. Comparison plots of the measured coupled power for the embedded antennas, foam thickness of 10 and 60 mm. Note that the maximum coupled power used for normalization was -44.4 dB.

## CONCLUSIONS

New advances in wireless sensors for structural health monitoring applications were presented. A new type of tunable helical resonator for strain measurements was shown. This resonator is capable of being tuned to the desired frequency of operation and provide higher resolution compared with other available cavity resonators. Next, a study of embedded antennas was presented. It was found that embedding a radiator will significantly distort its radiation pattern and lower the gain (lower signal levels at the DAU). Placing a foam cover layer on the antenna will improve the gain. However, the distortion in the pattern is still visible. Testing of the fabricated antennas verified the simulated data. As expected, the antenna with larger foam cover had higher gain values. From the fabrication data, it is evident that the designed antennas are suitable for embedding in concrete. The measured power of the antennas were high enough to be used with the passive wireless sensors.

## ACKNOWLEDGEMENT

The authors would like to thank ISIS Canada research network, the Natural Sciences and Engineering Research Council of Canada, and the University of Manitoba for their financial support.

## REFERENCES

1. G. Watter, P. Jayaweera, A. J. Bahr, and D. L. Huestis, "Design and Performance of Wireless Sensors For structural Health Monitoring", SRI international, 333 Ravenswood Ave., Menlo Park, CA 94025-3493, USA
2. Thorsten Sokoll and Arne F. Jacob, "A self-calibrating low-cost sensor system for moisture monitoring of buildings", 2006 IEEE
3. Carkhuff, B.; Cain, R., "Corrosion Sensors for Concrete Bridges", IEEE Instrumentation and Measurement Magazine, Volume 6, Issue 2, June 2003 pp. 19 - 24
4. A. Hladko, R. Jayas, D.J. Thomson and G.E. Bridges, "Development of a field usable interrogation system RF cavity wireless sensors", Proc. 3rd Intl. Conf. Bridge Safety and Management, Porto, Portugal, July 2006, pp. 1001-1003
5. Amara Loulizi, "Development of Ground Penetrating Radar Signal Modeling and Implementation for Transportation Infrastructure Assessment", Ph.D. Thesis, Virginia Polytechnic Institute, 2001.